

© 2016, Elsevier. Licensed under the Creative Commons Attribution-NonCommercial-NoDerivatives 4.0 International
<http://creativecommons.org/licenses/by-nc-nd/4.0/>

Accepted Manuscript

Representing spray zone with cross flow as a well-mixed compartment in a high shear granulator

Xi Yu, Michael J. Hounslow, Gavin K. Reynolds

PII: S0032-5910(16)30221-2
DOI: doi: [10.1016/j.powtec.2016.04.053](https://doi.org/10.1016/j.powtec.2016.04.053)
Reference: PTEC 11640

To appear in: *Powder Technology*

Received date: 31 October 2015
Revised date: 1 April 2016
Accepted date: 30 April 2016

Please cite this article as: Xi Yu, Michael J. Hounslow, Gavin K. Reynolds, Representing spray zone with cross flow as a well-mixed compartment in a high shear granulator, *Powder Technology* (2016), doi: [10.1016/j.powtec.2016.04.053](https://doi.org/10.1016/j.powtec.2016.04.053)

This is a PDF file of an unedited manuscript that has been accepted for publication. As a service to our customers we are providing this early version of the manuscript. The manuscript will undergo copyediting, typesetting, and review of the resulting proof before it is published in its final form. Please note that during the production process errors may be discovered which could affect the content, and all legal disclaimers that apply to the journal pertain.

Representing Spray Zone with Cross Flow as a Well-mixed Compartment in a High Shear Granulator

Xi Yu^{1,2,*}, Michael J. Hounslow², Gavin K. Reynolds³

1 European Bioenergy Research Institute (EBRI), School of Engineering and Applied Science, Aston University, Birmingham B4 7ET, UK

2 Department of Chemical and Biological Engineering, the University of Sheffield, Sheffield, S1 3JD, UK

3 Pharmaceutical Development, AstraZeneca, Macclesfield, SK10 2NA, UK

* Corresponding author. Email: x.yu3@aston.ac.uk

Keywords: High shear granulation, Spray zone, Well-mixed compartment

Abstract

The spray zone is an important region to control nucleation of granules in a high shear granulator. In this study, a spray zone with cross flow is quantified as a well-mixed compartment in a high shear granulator. Granulation kinetics are quantitatively derived at both particle-scale and spray zone-scale. Two spatial decay rates, DGSDR (droplet-granule spatial decay rate) ζ_{DG} and DPSDR (droplet-primary particle spatial decay rate) ζ_{DP} , which are functions of volume fraction and diameter of particulate species within the powder bed, are defined to simplify the deduction. It is concluded that in cross flow, explicit analytical results show that the droplet concentration is subject to exponential decay with depth which produces a numerically infinite depth spray zone in a real penetration process. In a well-mixed spray zone, the depth of the spray zone is $4/(\zeta_{DG} + \zeta_{DP})$ and $\pi^2/3(\zeta_{DG} + \zeta_{DP})$ in cuboid and cylinder shape, respectively. The first-order droplet-based collision rates of, nucleation rate B^0 and rewetting rate R_W^0 are uncorrelated with the flow pattern and shape of the spray zone. The second-order droplet-based collision rate, nucleated granule-granule collision rate R_{GG} , is correlated with the mixing pattern. Finally, a real formulation case of a high shear granulation process is used to estimate the size of the spray zone. The results show that the spray zone is a thin layer at the powder bed surface. We present, for the first time, the spray zone as a well-mixed compartment. The granulation kinetics of a

well-mixed spray zone could be integrated into a Population Balance Model (PBM), particularly to aid development of a distributed model for product quality prediction.

1. Introduction

Granulation is a particle production process that allows the design of products by varying the formulation of feeding materials and operating parameters. A series of different types of granulator such as tumbling drum, fluidized bed and high shear granulator are available, and the corresponding operating parameters are optimized to produce granules with desired properties. The research of this area over the last few decades of the 20th Century has been reviewed by Iveson et al [1]. Recent development of granulation technique can be seen (e.g. [2], [3], [4], [5], [6], [7], [8], [9], [10], [11]). From a modeller's point of view, the advance of multiscale modelling cannot be separated from the recent developments of measurement techniques (e.g. [2], [7]), understanding of granulation mechanism (e.g. [4], [5]) and optimal granulator design (e.g. [6], [8]). Advanced measurement methods can support researchers in identifying and optimising operating conditions, and selection of an appropriate mixer for the manufacturing of formulations. For example, Dale et al [2] presented X-ray microtomography techniques to non-destructively identify and describe spatial distributions of particle, binder, and air volumes within wet-granulated granules. Barling et al [7] proposed a novel experiment method to quickly and effectively evaluate the progression of dry powder mixing using a mixing-sensitive coloured tracer powder. The reliable identification of granulation mechanisms can advance researchers' understanding of the fundamental process to control granulation behaviour and product properties. For example, Tan and Hapgood [4] presented a regime map by plotting impeller speed, foam quality, and liquid to solid ratio to describe the granulation mechanisms for the foam and spray systems and the regime map provides a basis to customize formulations in achieving uniform

liquid distribution in a high-shear mixer-granulator. Charles-Williams et al [5] proposed new nucleation and granulation mechanism for granulation of mixtures of hydrophilic and hydrophobic components based on the experimental results on the granulation of mixtures of hydrophilic Granulac230 and hydrophobic limestone. Optimal granulator design may maximize the quality of granular product; meanwhile minimize the economic cost and environmental impact. For example, Mangwandi et al [6] found that the granulator fill factor has a profound effect on the compaction properties of the granules. Those produced from smaller batch sizes have superior compaction properties than those from larger batches. Granule batch size affects the strength and dissolution of the tablets formed. The tablets produced from large batches were found to be weaker and had a faster dissolution rate. Chan et al [8] utilized discrete element model (DEM) numerical technique to investigate horizontal high shear mixer flow behaviour and implications for scale-up. The DEM simulation can overcome the disadvantage of experimental method to predict and maintain the powder bed internal flow or stress field across scales during scaling up process.

The spray zone concept finds application in a wide range of granulators including fluidized bed, high shear mixer or similar devices. The studies of agglomerate formation reveal that product quality can be controlled by changing process parameters which in turn impact critical mechanisms in the spray zone of the fluidized drum granulator [12]. An exploratory surface energy-based spray zone concept has been used to describe surface energy changes of particles traversing the spray zone in a fluidized bed [13]. A novel nucleation apparatus for regime separated granulation was developed to produce narrow sized nuclei from various powder and binder liquid combinations [14]. In this design, the nucleation mechanism is completely separated from all other granulation mechanisms due to the lack of further mechanical mixing of the powder bed, which realizes the idealization of the spray zone as a plug flow

reactor. The excellent agreement of agglomerate formation data sets between mixed granulators [15] and ex-granulators [16] demonstrates that the ex-granulator experiments using a spinning riffler under a plug flow field do effectively mirror the spray zone in a mixer granulator.

The spray zone is a special zone with relatively well defined flow field and spatial-preferred transformation kinetics in a granulator. The qualitative definition of the nucleation zone [1] was given to describe the first contact between the powder surface and liquid binder to form the initial nuclei granules which is an important process that dominates in this compartment in the early stages of granulation. Hapgood et al ([16], [17]) demonstrated the critical importance of the nucleation and liquid binder distribution process in determining the size and spread of the final granule size distribution.

All previous literature qualitatively describes the spray zone or develops a micro-scale transformation model to characterize mechanisms occurring in the spray zone. Although some mesoscale model of wet granulation have been done (e.g. [18] [19]), there is a lack of mesoscopic model to link microscopic models and macroscopic models (e.g. Population Balance Model [20] [21]) in describing granulation rates, such as nucleation, in a spray zone. The significance of developing mesoscopic models has been addressed by Michaels [22] in particulate systems. Therefore, in this study, we aim to develop a mesoscopic model of the spray zone in high shear granulator

- I. to quantify transformation kinetics and transport phenomena in the spray zone
- II. to determine the size of spray zone and estimate volume averaged granulation rates for Population Balance Model
- III. to link microscopic models and macroscopic models

The paper is a mathematical model for the spray zone that allows its estimation from measurable variables.

1.1. Shape of spray zone

The location of a spray zone is beneath the spraying nozzle and on the surface of powder bed. The nozzle position (height above powder bed) and the spray angle are commonly used to alter the size of the spray zone [1], which means the bed surface area of the spray zone (in x and y coordinates in Fig. 1) is determined by the design and feature of the nozzle. The location and shape of a nucleation zone has been discussed by Iveson et al [1]. There are three common spray types: flat, circular and annular; in this study, we investigate cuboid and cylindrical shapes to correspond to flat and circular spray conditions, respectively. Therefore, two geometric shapes (cuboid in Fig. 1a and cylinder Fig. 1b) of the spray zone are considered in the model. In a realistic granulation process, the powder bed will be close to a cross flow arrangement with respect to binder penetration within the spray zone as described in section 2.2.

1.2. Interaction

The interactions among three different particulate species: droplet (liquid binder), primary particle (dry powder) and granule in the spray zone of high shear granulator are addressed in this section. As liquid binder is sprayed on the powder bed surface and penetrates into the powder bed, there are three possible interactions occurring within spray zone including nucleation, rewetting and nucleated granule-granule collision in Fig. 2.

In order to derive analytical solutions of the mathematical model in section 2, reasonable assumptions, based on physical phenomena, are listed as following

- (1) Droplet-controlled nucleation [1] occurs in the spray zone. That is to say, one droplet forms a nucleus. Droplet can exist only in the spray zone.
- (2) Primary particles are smaller than the droplets in this case. The kinetics of nucleation (Fig. 2) is treated as an immersion mechanism [23].

- (3) The rewetting (Fig. 2) occurs when a droplet collides with an existing granule and the droplet is absorbed by the granule.
- (4) The collision kernel is based on the binary collision rate of a fast moving droplet (sprayed from the nozzle) collided with a slow moving particle (primary particle or granule).
- (5) The deduction is at steady state, and the concentration (number density) of primary particles and existing granules are assumed to be constant.
- (6) Nucleated granule-granule collision (Fig. 2): the colliding of two granule nuclei tends to coalesce. Nucleated granule-granule collision rate is treated as a second-order function of droplet concentration. Successful collisions are able to increase the effective nuclei size, which is similar to the coalescence of droplets at the powder bed surface.
- (7) As we assume droplet controlled nucleation occurs in the spray zone (mentioned in the assumption 1) in which nucleation regime, one drop tends to form one granule as the spray droplets penetrate quickly into the powder and are well dispersed. Therefore, in this study, it is reasonable to ignore droplet-droplet collisions and mutual collisions of wet granules after rewetting as the binder droplet are well dispersed. In real wet high shear granulation process, the probability of droplet-droplet collisions and the mutual collisions of wet granules after rewetting is ignorable low if the optimal operation is realized by controlling nucleation process to occur at drop controlled regime in nucleation regime map [17].

2. Model

2.1. Mass balance

In this section, a theoretical mathematical model based on the mass balance of droplet (liquid binder), granule and primary particle (dry powder) in the spray zone of high shear granulator is developed.

The mass balance of the droplet, granule and primary particle at steady state respectively are

$$\nabla(\vec{U}_D N_D) + r_{DP} + r_{DG} = 0 \quad (1a)$$

$$\nabla(\vec{U}_G N_G) - r_{DP} = 0 \quad (1b)$$

$$\nabla(\vec{U}_P N_P) - r_{DP} \frac{D_D^2}{D_P^2} = 0 \quad (1c)$$

\vec{U}_D is velocity vector of the droplets, \vec{U}_G and \vec{U}_P are velocity vector of the granules and primary particles, respectively, in this study, $\vec{U}_G = \vec{U}_P$, N_D is number density of the droplets, r_{DP}, r_{DG} are nucleation rate and rewetting rate per unit volume, respectively. Subscripts G, P and D represent granule, primary particle and droplet respectively.

The definition of nucleated granule is: a core droplet with one uniform monolayer of primary particles. So the nucleation rate and rewetting rate are defined as

$$r_{DP} = \beta_{DP} N_P N_D \frac{D_P^2}{D_D^2} \quad (2a)$$

$$r_{DG} = \beta_{DG} N_G N_D \quad (2b)$$

β_{DP}, β_{DG} are the collision kernels of the droplet-granule collision and droplet-primary particle collision, respectively. N_G, N_P are the number densities of the granules and primary particles, respectively. D_P, D_D are the diameters of the primary particle and droplet, respectively. The factor D_D^2/D_P^2 is used to describe the “coating” phenomena, giving the number of primary particles covering the surface of one droplet.

Based on the hypothesis (4) in section 1.2, collision kernels of nucleation and rewetting are defined as

$$\beta_{DP} = \frac{\pi}{4} U_D (D_D + D_P)^2 \quad (3a)$$

$$\beta_{DG} = \frac{\pi}{4} U_D (D_D + D_G)^2 \quad (3b)$$

D_G is the diameter of the granule

Liquid droplets are assumed to fall vertically on the surface of a powder bed with uniform velocity $\vec{U}_D = (0, 0, U_D)$. Then, combining Eq. 2b and 3b to give

$$r_{DG} = \frac{\pi}{4} U_D (D_D + D_G)^2 N_G N_D \quad (4a)$$

Combining Eq. 2a and 3a to give

$$r_{DP} = \frac{\pi}{4} U_D (D_D + D_P)^2 N_P N_D \frac{D_P^2}{D_D^2} \quad (4b)$$

Based on a one dimensional constant-velocity assumption of droplet penetration into a powder bed in cross flow, Eq.1 is simplified into a one dimensional equation

$$U_D \frac{dN_D}{dz} + r_{DP} + r_{DG} = 0 \quad (5)$$

2.2. Cross flow

2.2.1. Cuboid spray zone

Combining Eq. 4a-b and 5 to give N_D as a function of z

$$N_D(z) = N_D(0) e^{-\frac{\pi z (D_D^2 (D_D + D_G)^2 N_G + D_P^2 (D_D + D_P)^2 N_P)}{4 D_D^2}} \quad (6)$$

$N_D(0)$ is the number density of the droplets at the surface of powder bed, $z = 0$. To simplify Eq. 6, we attempt to replace the number density N by using the volume fraction ε . The voidage of the powder bed ε_A can be measured directly [24] or computed from experimented measurements [25].

Since ε_A is known, the correlations between volume fraction ε , diameter D and number of granules per volume N are

$$\pi D_G^3 N_G / 6 = \varepsilon_G \quad (7a)$$

$$\pi D_P^3 N_P / 6 = \varepsilon_P \quad (7b)$$

$$\varepsilon_G + \varepsilon_P + \varepsilon_A = 1 \quad (7c)$$

Since the assumption (1) states that droplet controlled nucleation occurs in the spray zone, in which nucleation regime, the ratio t_p/t_c is <0.1 , that means the drop penetration time (t_p) is much shorter compared to particle circulating time (t_c). It explained that droplets penetrate quickly into the powder, therefore, after a very short period of time (t_p), the droplets exist as nuclei core of the granules. Thus, in Eq. (7C)

and (44b), it is reasonable to neglect volume fraction of droplets not consumed by granules.

To simplify Eq.6, two new variables DGSDR (droplet-granule spatial decay rate) ζ_{DG} and DPSDR (droplet-primary particle spatial decay rate) ζ_{DP} are defined as

$$(D_D + D_G)^2 \frac{\varepsilon_G}{D_G^3} = \zeta_{DG} \quad (8a)$$

$$(D_D + D_P)^2 \frac{\varepsilon_P}{D_D^2 D_P} = \zeta_{DP} \quad (8b)$$

Combining Eq. 6, 7a-b and 8a-b gives

$$N_D(z) = N_D(0) e^{-\frac{3}{2}z(\zeta_{DG} + \zeta_{DP})} \quad (9)$$

As described in hypothesis (5) in section 1.2, the change of N_G and N_P is negligible at steady state, which is true particularly in the early stage of nucleation in the real granulation process, therefore N_G and N_P are assumed to be constant. Eq. 9 shows that the concentration of droplets is subject to exponential decay, which means $N_D(z)$ decreases at a rate (spatially) proportional to its value:

$$\frac{dN_D}{dz} = -\lambda N_D \quad (10a)$$

$$\lambda = \frac{3}{2} (\zeta_{DG} + \zeta_{DP}) \quad (10b)$$

Where λ is the decay constant. Based on the Eq. 9, it is concluded that the mathematical depth of a spray zone is infinite.

After derivation of $N_D(z)$ in Eq 9, N_G in Eq.1b is examined as below.

As the plug flow of the powder bed is used, Eq.1b is simplified into

$$U_G \frac{dN_G}{dx} - r_{DP} = 0 \quad (11)$$

U_G is moving at the velocity of the powder bed. Combining Eq. 9 and 11 to give

$$N_G(x, z) = N_G(0) + \frac{3x\zeta_{DP}N_D(0)U_D e^{-\frac{3}{2}z(\zeta_{DG} + \zeta_{DP})}}{2U_G} \quad (12)$$

$N_G(0)$ is the number density of the granules located at the boundary where granules are moving in the spray zone, $x = 0$.

The total nucleation rate is the total number of increments per second in the spray zone

$$B^0 = U_G Y \left(\int_0^{+\infty} N_G(X) dz - \int_0^{+\infty} N_G(0) dz \right) = \frac{XY N_D(0) \zeta_{DP} U_D}{(\zeta_{DG} + \zeta_{DP})} \quad (13a)$$

To simplify Eq. 13a, the total feed rate of liquid binder into spray zone is defined as

$$R_D^0 = XY N_D(0) U_D \quad (13b)$$

So Eq. 13a is transformed to

$$B^0 = \frac{\zeta_{DP} R_D^0}{(\zeta_{DG} + \zeta_{DP})} \quad (13c)$$

The total rewetting rate is the total number of droplets consumed by existing granules in spray zone per second

$$R_W^0 = R_D^0 - B^0 = \frac{\zeta_{DG} R_D^0}{(\zeta_{DG} + \zeta_{DP})} \quad (14)$$

The concentration of nucleated granules is the increment of granule concentration in the spray zone from Eq. 12

$$N_G^* = N_G(x) - N_G(0) = \frac{3x \zeta_{DP} N_D(0) U_D e^{-\frac{3}{2}z(\zeta_{DG} + \zeta_{DP})}}{2U_G} \quad (15)$$

Eq 15 shows that N_G^* not only decays exponentially with z , but also increases linearly with x .

If nucleated granule-granule collision occur as hypothesis (6) in section 1.2, even if very small compared with as the second-order rate of droplet concentration, it can be defined as

$$r_{GG} = \beta_{GG} N_G^{*2} \quad (16)$$

The total nucleated granule-granule collision rate in the spray zone is

$$R_{GG} = \int_0^{+\infty} \int_0^Y \int_0^X r_{GG} dx dy dz = -Y \beta_{GG} \frac{a^2 X^3}{6b} \quad (17a)$$

$$a = \frac{3\zeta_{DP} N_D(0) U_D}{2U_G}, b = -\frac{3}{2}(\zeta_{DG} + \zeta_{DP}) \quad (17b)$$

Combining Eq.17a and 17b to give

$$R_{GG} = \frac{X \beta_{GG} (\zeta_{DP} R_D^0)^2}{4(\zeta_{DG} + \zeta_{DP}) Y U_G^2} \quad (18)$$

2.2.2. Cylindrical spray zone

The geometry change of the spray zone has no effect on the distribution of droplet concentration along the z direction in Eq. 9. The concentration increment of granules $N_G(x)$ is a function of distance x away from the granule inflow boundary (Eq. 12). The top view of the spray zone in a cylindrical geometry is shown in Fig.3. Point A is an arbitrary spatial position located at the spray zone, x is the distance away from the inlet boundary along powder bed movement, θ is the angle from the positive x axis, R is the radius of the cylinder geometry and r is the distance away from the central axis.

x is calculated using triangular relationship

$$x = \sqrt{R^2 - r^2 \sin^2 \theta} - r \cos \theta \quad (19)$$

when $r = R$ at the boundary of the spray zone

$$x = R(|\cos \theta| - \cos \theta) \quad (20)$$

when $-\frac{\pi}{2} < \theta < \frac{\pi}{2}$ & $r = R$ at the borders of the spray zone where granules are entering, the number density of granules is

$$N_G(\theta) = N_G \quad (21a)$$

When $\frac{\pi}{2} < \theta < \frac{3\pi}{2}$ & $r = R$ at the borders of the spray zone where granules are moving out, the number density of the granules is

$$N_G(\theta) = N_G + \frac{-3R \cos \theta \zeta_{DP} N_D(0) U_D e^{-\frac{3}{2}z(\zeta_{DG} + \zeta_{DP})}}{U_G} \quad (22b)$$

The total nucleation rate of the spray zone is

$$\begin{aligned} B^0 &= U_G R \left(\int_{\frac{\pi}{2}}^{\frac{3\pi}{2}} \int_0^{+\infty} -N_G(\theta) \cos \theta dz d\theta - \int_{-\frac{\pi}{2}}^{\frac{\pi}{2}} \int_0^{+\infty} -N_G(\theta) \cos \theta dz d\theta \right) \\ &= \frac{\zeta_{DP} R_D^0}{(\zeta_{DG} + \zeta_{DP})} \end{aligned} \quad (23a)$$

The total rewetting rate of the spray zone is

$$R_W^0 = R_D^0 - B^0 = \frac{\zeta_{DG} R_D^0}{(\zeta_{DG} + \zeta_{DP})} \quad (23b)$$

The total nucleated granule-granule collision of the spray zone is

$$R_{GG} = \int_0^{+\infty} \int_{-\pi/2}^{3\pi/2} \int_0^R r_{GG} r dr d\theta dz = -\beta_{GG} \frac{\pi a^2 R^4}{2b} \quad (24a)$$

$$a = \frac{3\zeta_{DP} N_D(0) U_D}{2U_G}, b = -\frac{3}{2}(\zeta_{DG} + \zeta_{DP}) \quad (24b)$$

Combining Eq. 24a and 24b to obtain

$$R_{GG} = \frac{3\beta_{GG}(\zeta_{DP} R_D^0)^2}{4\pi(\zeta_{DG} + \zeta_{DP})U_G^2} \quad (25)$$

2.3. Well-mixed flow

2.3.1. Cuboid spray zone

A well-mixed spray zone in a cuboid geometry is shown in Fig 4. The concentration of any species is constant in the well-mixed spray zone.

The mass balance of the droplets is

$$R_D^0 = XYZ(r_{DP} + r_{DG}) \quad (26)$$

Where Z is the depth of the well-mixed spray zone. Combining Eq. 4a-b, 7a-b and 8a-b gives the ratio of r_{DP} to r_{DG}

$$\frac{r_{DP}}{r_{DG}} = \frac{\zeta_{DP}}{\zeta_{DG}} \quad (27)$$

Eq. 27 reveals that the ratio is uncorrelated with the flow pattern (cross flow or well-mixed flow) and does not depend on the size of the spray zone.

Combining Eq. 26 and 27 gives

$$B^0 = XYZ r_{DP} = \frac{\zeta_{DP} R_D^0}{\zeta_{DG} + \zeta_{DP}} \quad (28a)$$

$$R_W^0 = XYZ r_{DG} = \frac{\zeta_{DG} R_D^0}{\zeta_{DG} + \zeta_{DP}} \quad (28b)$$

By comparing Eq. 13c, 14 and 28a-b, the consistent formulas show that B^0 and R_W^0

are not correlated with the flow pattern (cross flow or well-mixed flow). First-order rates of droplet concentration (nucleation and rewetting rates) are not able to determine the size of well-mixed spray zone.

Combining Eq. 4a-b, 7a-b, 8a-b and 26 gives

$$N_D = \frac{2R_D^0}{3XYZU_D(\zeta_{DG} + \zeta_{DP})} \quad (29)$$

To estimate depth of spray zone Z in Eq. 29, nucleated granule-granule collision is estimated in the well-mixed spray zone.

The mass balance of granules in the spray zone is

$$N_G^*Q = XYZr_{DP} \quad (30)$$

Where Q is volume flow rate of powder bed moving into spray zone, Combining Eq. 28a and 30 gives

$$N_G^* = \frac{\zeta_{DP}R_D^0}{(\zeta_{DG} + \zeta_{DP})Q} \quad (31)$$

Using the definition of r_{GG} in Eq. 16, R_{GG} is

$$R_{GG} = XYZ\beta_{GG} \left(\frac{\zeta_{DP}R_D^0}{(\zeta_{DG} + \zeta_{DP})Q} \right)^2 \quad (32)$$

A well-mixed spray zone with volume XYZ to represent the real spray zone with cross flow requires the same R_{GG} in both flow patterns in Eq. 18 and 32 as below

$$XYZ\beta_{GG} \left(\frac{\zeta_{DP}R_D^0}{(\zeta_{DG} + \zeta_{DP})Q} \right)^2 = \frac{X\beta_{GG}(\zeta_{DP}R_D^0)^2}{4(\zeta_{DG} + \zeta_{DP})YU_G^2} \quad (33)$$

Continuing to simplify Eq. 33, the depth of the well-mixed spray zone is

$$Z = \frac{(\zeta_{DG} + \zeta_{DP})Q^2}{4Y^2U_G^2} \quad (34)$$

The flow rate of powder bed at the inlet boundary of the well-mixing spray zone $Q = YZU_G$, then Eq. 34 is transformed into

$$Z = \frac{4}{(\zeta_{DG} + \zeta_{DP})} \quad (35)$$

2.3.2. Cylindrical spray zone

A well-mixed spray zone in a cylindrical geometry is shown in Fig. 5.

The mass balance of the droplets is

$$R_D^0 = \pi R^2 Z (r_{DP} + r_{DG}) \quad (36)$$

Combining Eq. 27 and 36 gives

$$B^0 = \pi R^2 Z r_{DP} = \frac{\zeta_{DP} R_D^0}{\zeta_{DG} + \zeta_{DP}} \quad (37a)$$

$$R_W^0 = \pi R^2 Z r_{DG} = \frac{\zeta_{DG} R_D^0}{\zeta_{DG} + \zeta_{DP}} \quad (37b)$$

The mass balance of granules in the spray zone is

$$N_G^* Q = \pi R^2 Z r_{DP} \quad (38)$$

Combining Eq. 37a and 38 to give

$$N_G^* = \frac{\zeta_{DP} R_D^0}{(\zeta_{DG} + \zeta_{DP}) Q} \quad (39)$$

Using the definition of r_{GG} in Eq. 23a, R_{GG} is

$$R_{GG} = \pi R^2 Z \beta_{GG} \left(\frac{\zeta_{DP} R_D^0}{(\zeta_{DG} + \zeta_{DP}) Q} \right)^2 \quad (40)$$

A well-mixed spray zone with volume $\pi R^2 Z$ to represent spray zone with cross flow requires the same R_{GG} in both flow patterns in Eq. 25 and 40 as below

$$\pi R^2 Z \beta_{GG} \left(\frac{\zeta_{DP} R_D^0}{(\zeta_{DG} + \zeta_{DP}) Q} \right)^2 = \frac{3 \beta_{GG} (\zeta_{DP} R_D^0)^2}{4 \pi (\zeta_{DG} + \zeta_{DP}) U_G^2} \quad (41)$$

Continuing to simplify Eq. 41, the depth of the well-mixed spray zone is

$$Z = \frac{3(\zeta_{DG} + \zeta_{DP}) Q^2}{4 \pi^2 R^2 U_G^2} \quad (42)$$

The flow rate of powder bed at the inlet boundary of the well-mixing spray zone $Q = Z R U_G \int_{-\pi/2}^{\pi/2} \cos \theta d\theta = 2 Z R U_G$, then Eq. 42 is transformed into

$$Z = \frac{\pi^2}{3(\zeta_{DG} + \zeta_{DP})} \quad (43)$$

Comparing penetration depth in Eq. 35 and 43, the constant factor changes from 4 to $\pi^2/3$ by changing the shape of spray zone from cuboid to cylinder.

3. A typical formulation case

Since the formula (Eq. 35 and 43) for the size of a well-mixed spray zone is known, a real granulation case is used as an example to estimate the size of the spray zone.

The mass balance of the powder bed is

$$V\rho_{bulk} = V\frac{\pi D_G^3\rho_G N_G}{6} + V\frac{\pi D_P^3\rho_P N_P}{6} + V\varepsilon_A\rho_A \quad (44a)$$

ρ_{bulk} is bulk density of powder bed, V is volume of powder bed

Simplifying Eq. 44a into,

$$\rho_{bulk} = \varepsilon_G\rho_G + \varepsilon_P\rho_P + \varepsilon_A\rho_A \quad (44b)$$

The density of air is negligible relative to that of the powder bed, so $\varepsilon_A\rho_A/\rho_{bulk} \rightarrow 0$, and Eq. 44b is changed into

$$\rho_{bulk} = \varepsilon_G\rho_G + \varepsilon_P\rho_P \quad (44c)$$

Before granulation, the bulk density for a dry powder bed is

$$\rho_{bulk} = \varepsilon_P\rho_P \quad (45a)$$

After granulation, the bulk density for a wet powder bed is

$$\rho_{bulk} = \varepsilon_G\rho_G \quad (45b)$$

The bulk density of powder bed and granule (or primary particle) apparent density are able to be measured separately using the method given by Hinkley et al [25]. To roughly estimate the depth of well-mixed spray zone, we give a rational guess on the assumption that the volume fractions of both solid species are the same at the moment of granulation process. The porosity of the powder bed is 0.6. To validate the mathematical model and explore the real size of spray zone in wet high shear granulation, we utilize the experimental data of real wet high shear granulation [26] to replace all variables (e.g. particle size and volume fraction) in equation 35 and 43, thus estimate the size of spray zone in cuboid and cylinder shape. The chosen granulation experiment was conducted to granulate a mixture (calcium phosphate, microcrystalline cellulose, povidone and crospovidone) with water using a 10L Rotojunior mixer (Zanchetta, Italy). We mathematically calculate the drop penetration time as below [17]

$$t_p = 1.35 \frac{V_0^{2/3}}{\varepsilon^2 R_{pore}} \frac{\mu}{\gamma_{LV} \cos \theta_d} \quad (46)$$

$$R_{pore} = \frac{2\varepsilon}{(1-\varepsilon)S_0\rho_s} \quad (47)$$

The t_p is approximate 5.19×10^{-2} s when the variables in above equation are substituted with practical constant as: V_0 is the total drop volume, $10\mu L$. ε is surface porosity, 0.45. R_{pore} is effective pore radius based on cylindrical pores, m. S_0 is the particle specific surface area, $60 \text{ m}^2/\text{kg}$. ρ_s is powder density, 1500 kg/m^3 . μ is viscosity, $1.1 \text{ mPa}\cdot\text{s}$. γ_{LV} is the liquid surface tension, 72.1 mN/m . θ_d is the solid-liquid contact angle, 60 degree.

Currently, there is no theoretical formula to calculate the particle circulation time (t_c), however, Ng et al [27] utilized positron emission particle tracking (PEPT) technique to successfully obtain vertical circulation period, which is defined as the time taken by the tracer particle to move from a position higher than an upper boundary in the high shear granulator and return to the upper part of the mixer. When the high shear granulator operated at 3.9Hz of impeller speed, the range of vertical circulation period is from 1.92s to 43.86 in dry condition and from 4.58s to 42.69s in wet condition, respectively. Back to the granulation case used in this study, the high shear granulator operated at 4Hz of impeller speed, therefore, it is confident to deduce that the particle circulation time should be at the same time scale $1\sim 10\text{s}$, so the ratio t_p/t_c is <0.1 .

Then we calculate the dimensionless spray flux Ψ_a as below [16]

$$\Psi_a = \frac{3\dot{V}}{2\dot{A}D_D} \quad (48)$$

The Ψ_a is approximate 0.074 when the variables in above equation are substituted with practical constant as: \dot{V} is volumetric spray rate, $3.7 \times 10^{-6} \text{ m}^3/\text{s}$, \dot{A} is the powder flux $0.15 \text{ m}^2/\text{s}$. D_D is the drop diameter, 0.5mm .

We can be confident that the assumption of drop controlled nucleation is valid in the granulation case chosen. To calculate the size of the spray zone, the variables in equation 35 and 43 are substituted with practical constants of experimental data [26]

as listed in Table 1. The typical values of spray zone depths are 0.433mm in cuboid shape and 0.356mm in cylindrical shape respectively with mean sizes of particle species (droplet, primary particle and granule). The maximum value of spray zone depths are 1.317 in cuboid shape and 1.084 mm in cylindrical shape respectively with maximum sizes of particle species. From numerical point of view, the depth of spray zone is approximate 10 times of droplet size. It is the first time to quantify this size via a mathematical model for the spray zone that allows its estimation from measurable variables.

The successful derivation of size of well mixed spray zone makes it possible to develop a compartmental PBM [20], which can integrate the microscopic mechanisms (e.g. nucleation and rewetting) in spray zone into a macroscopic model. For example, Yu [20] has developed a compartmental PBM model including spray zone and utilized computation fluid dynamics (CFD) to simulate gas-solid flow in high shear granulator and numerically predict the flow flux of granules flowing in and out the spray zone, which depth was assumed to 5~10 times of the mesh size used in CFD. In this study, the result in Table 1 shows the depth of spray zone is approximate 10 times of droplet size, however, in practise, such as CFD simulation, it is challenge to obtain correct numerical flow flux in/out the spray zone if using 10 times of droplet size (e.g. 1~2 mm). Therefore, in further application (e.g. PBM) of depth of the spray zone based on the conclusion of this study, the authors recommend suitable adjustment (such as 5~10 times of mesh size in CFD) of spray zone to match the requirement of compartmental PBM.

In this study, the size of spray zone is determined based on the hypothesis that drop controlled nucleation occurs in the spray zone. If nucleation occurs at other regimes, the size of spray zone is also subject to liquid material and the wetting rate.

4. Conclusion

The spray zone with cross flow is quantified as a well-mixed compartment in a high shear granulator. Granulation kinetics are quantitatively estimated at both particle-scale and spray zone-scale. Two spatial decay rates, DGSDR (ζ_{DG}) and DPSDR (ζ_{DP}), which are functions of volume fraction and diameter of particulate species within the powder bed, are defined to simplify the deduction.

- 1) In cross flow, explicit analytical results show that the droplet concentration is subject to exponential decay with depth which produces a numerically infinite depth spray zone in a real penetration process.
- 2) In a well-mixed spray zone, the depths of the spray zones are $4/(\zeta_{DG} + \zeta_{DP})$ and $\pi^2/3(\zeta_{DG} + \zeta_{DP})$ in cuboid and cylinder shape, respectively.
- 3) The first-order droplet-based collision rate, nucleation rate B^0 and rewetting R_W^0 are uncorrelated with the flow pattern and shapes of the spray zone.
- 4) The second-order droplet-based collision rate, nucleated granule-granule collision rate, R_{GG} is correlated with the mixing pattern.
- 5) A real formulation case for high shear granulation combined with a reasonable estimate of voidages of particulate species within the powder bed is provided to estimate the size of the spray zone. The results show that the spray zone is a thin layer at the powder bed surface.

We present, for the first time, the spray zone as a well-mixed compartment. The granulation kinetics of a well-mixed spray zone could be integrated into PBM, particularly to aid development of a distributed model for product prediction.

Acknowledgment

The authors are grateful to AstraZeneca for funding

Nomenclature

Roman symbols

a Parameter (m^{-4})

\dot{A}	Powder flux (m^2s^{-1}).
b	Parameter (m^{-1})
B^0	Total nucleation rate (s^{-1})
D	Diameter (m)
N	Number Density ($\# \text{m}^{-3}$)
N_G^*	Concentration of nucleated granules ($\# \text{m}^{-3}$)
Q	Volume flow rate ($\text{m}^3 \text{s}^{-1}$)
r	Distance away from the central axis (m)
r_{DP}	Nucleation rate per volume unit ($\text{m}^{-3} \text{s}^{-1}$)
r_{DG}	Rewetting rate per volume unit ($\text{m}^{-3} \text{s}^{-1}$)
r_{GG}	Collision rate between nucleated granules ($\text{m}^{-3} \text{s}^{-1}$)
R	Radius of the cylinder geometry (m)
R_D^0	Total feed rate of liquid binder (s^{-1})
R_{GG}	Total collision rate between nucleated granules ($\text{m}^{-3} \text{s}^{-1}$)
R_{pore}	Effective pore radius based on cylindrical pores (m)
R_W^0	Total rewetting rate (s^{-1})
t_p	Drop penetration time (s)
t_c	the particle circulation time (s)
\vec{U}	Velocity vector (m s^{-1})
V_0	Drop volume (m^3)
V	Volume of powder bed (m^3)
\dot{V}	Volumetric spray rate (m^3s^{-1})
x, X	Length (m)
y, Y	Length (m)
z, Z	Depth (m)

Greek symbols

β	Collision kernel ($\text{m}^3 \text{s}^{-1}$)
γ_{LV}	Liquid surface tension (N m^{-1}).
ε	Volume fraction (—)
ζ	Spatial decay rate (m^{-1})
θ	Angle from the positive x axis (rad)
θ_d	Solid-liquid contact angle (rad).
λ	Decay constant (m^{-1})
μ	Viscosity (Pa.S).
ρ	Density (kg m^{-3})
Ψ_a	Dimensionless spray flux (—)

Subscripts

0	Initial, i.e., at $t = 0$.
A	Air
G	Granule
P	Primary particle

D Droplet

References

- [1] S.M. Iveson, J.D. Litster, K. Hapgood, B.J. Ennis, Nucleation, growth and breakage phenomena in agitated wet granulation processes: a review, *Powder Technology*, 117 (2001) 3-39.
- [2] S. Dale, C. Wassgren, J. Litster, Measuring granule phase volume distributions using X-ray microtomography, *Powder Technology*, 264 (2014) 550-560.
- [3] A.S. El Hagrasy, J.D. Litster, Granulation rate processes in the kneading elements of a twin screw granulator, *AIChE Journal*, 59 (2013) 4100-4115.
- [4] M.X.L. Tan, K.P. Hapgood, Mapping of regimes for the key processes in wet granulation: Foam vs. spray, *AIChE Journal*, 59 (2013) 2328-2338.
- [5] H. Charles-Williams, R. Wengeler, K. Flore, H. Feise, M.J. Hounslow, A.D. Salman, Granulation behaviour of increasingly hydrophobic mixtures, *Powder Technology*, 238 (2013) 64-76.
- [6] C. Mangwandi, M.J. Adams, M.J. Hounslow, A.D. Salman, Influence of fill factor variation in high shear granulation on the post granulation processes: Compression and tablet properties, *Powder Technology*, 263 (2014) 135-141.
- [7] D. Barling, D.A.V. Morton, K. Hapgood, Pharmaceutical dry powder blending and scale-up: Maintaining equivalent mixing conditions using a coloured tracer powder, *Powder Technology*, 270, Part B (2015) 461-469.
- [8] E.L. Chan, K. Washino, H. Ahmadian, A. Bayly, Z. Alam, M.J. Hounslow, A.D. Salman, Dem investigation of horizontal high shear mixer flow behaviour and implications for scale-up, *Powder Technology*, 270, Part B (2015) 561-568.
- [9] T.C. Seem, N.A. Rowson, A. Ingram, Z. Huang, S. Yu, M. de Matas, I. Gabbott, G.K. Reynolds, Twin screw granulation — A literature review, *Powder Technology*, 276 (2015) 89-102.
- [10] S. Oka, H. Emady, O. Kašpar, V. Tokárová, F. Muzzio, F. Štěpánek, R. Ramachandran, The effects of improper mixing and preferential wetting of active and excipient ingredients on content uniformity in high shear wet granulation, *Powder Technology*, 278 (2015) 266-277.
- [11] R. Sayin, A.S. El Hagrasy, J.D. Litster, Distributive mixing elements: Towards improved granule attributes from a twin screw granulation process, *Chemical Engineering Science*, 125 (2015) 165-175.
- [12] J.D. Litster, R. Sarwono, Fluidized drum granulation: studies of agglomerate formation, *Powder Technology*, 88 (1996) 165-172.
- [13] D.K. Kafui, C. Thornton, Fully-3D DEM simulation of fluidised bed spray granulation using an exploratory surface energy-based spray zone concept, *Powder Technology*, 184 (2008) 177-188.
- [14] W.J. Wildeboer, E. Koppendraaier, J.D. Litster, T. Howes, G. Meesters, A novel nucleation apparatus for regime separated granulation, *Powder Technology*, 171 (2007)

96-105.

- [15] J.D. Litster, K.P. Hapgood, J.N. Michaels, A. Sims, M. Roberts, S.K. Kameneni, Scale-up of mixer granulators for effective liquid distribution, *Powder Technology*, 124 (2002) 272-280.
- [16] J.D. Litster, K.P. Hapgood, J.N. Michaels, A. Sims, M. Roberts, S.K. Kameneni, T. Hsu, Liquid distribution in wet granulation: dimensionless spray flux, *Powder Technology*, 114 (2001) 32-39.
- [17] K.P. Hapgood, J.D. Litster, R. Smith, Nucleation regime map for liquid bound granules, *AIChE Journal*, 49 (2003) 350-361.
- [18] D. Barrasso, R. Ramachandran, Multi-scale modeling of granulation processes: Bi-directional coupling of PBM with DEM via collision frequencies, *Chemical Engineering Research and Design*, 93 (2015) 304-317.
- [19] K. Washino, H.S. Tan, M.J. Hounslow, A.D. Salman, Meso-scale coupling model of DEM and CIP for nucleation processes in wet granulation, *Chemical Engineering Science*, 86 (2013) 25-37.
- [20] X. Yu, An in-silico model of granulation, University of Sheffield, PhD thesis, 2012.
- [21] X. Yu, M.J. Hounslow, G.K. Reynolds, Accuracy and optimal sampling in Monte Carlo solution of population balance equations, *AIChE Journal*, 61 (2015) 2394-2402.
- [22] J.N. Michaels, Toward rational design of powder processes, *Powder Technology*, 138 (2003) 1-6.
- [23] M.J. Hounslow, M. Oullion, G.K. Reynolds, Kinetic models for granule nucleation by the immersion mechanism, *Powder Technology*, 189 (2009) 177-189.
- [24] M.J. San José, M. Olazar, S. Alvarez, J. Bilbao, Local Bed Voidage in Conical Spouted Beds, *Industrial & Engineering Chemistry Research*, 37 (1998) 2553-2558.
- [25] J. Hinkley, A.G. Waters, D. O'Dea, J.D. Litster, Voidage of ferrous sinter beds: new measurement technique and dependence on feed characteristics, *International Journal of Mineral Processing*, 41 (1994) 53-69.
- [26] M. Oullion, G.K. Reynolds, M.J. Hounslow, Simulating the early stage of high-shear granulation using a two-dimensional Monte-Carlo approach, *Chemical Engineering Science*, 64 (2009) 673-685.
- [27] B.H. Ng, C.C. Kwan, Y.L. Ding, M. Ghadiri, X.F. Fan, Solids motion of calcium carbonate particles in a high shear mixer granulator: A comparison between dry and wet conditions, *Powder Technology*, 177 (2007) 1-11.

List of figures

Fig. 1 Schematic of the spray zone with cross flow in a (a) cuboid geometry (b) cylindrical geometry

Fig 2 Schematic of three particulate species and their interactions in the spray zone

Fig. 3 Top view of the spray zone with cross flow in a cylindrical geometry

Fig. 4 Schematic of the well mixed spray zone in a cuboid geometry

Fig 5 Schematic of the well-mixed spray zone in a cylindrical geometry

Table 1 The depth of the spray zone corresponding to particle size and volume fraction

Parameters	D_D (mm)	D_P (mm)	D_G (mm)	ε_G	ε_P	Z (cuboid) (mm)	Z (Cylinder) (mm)
Range	0.05-0.5	0.01-0.1	0.1-2	0.2	0.2		
Typical value	0.1	0.05	1			0.433	0.356
Max value	0.5	0.1	2			1.317	1.084

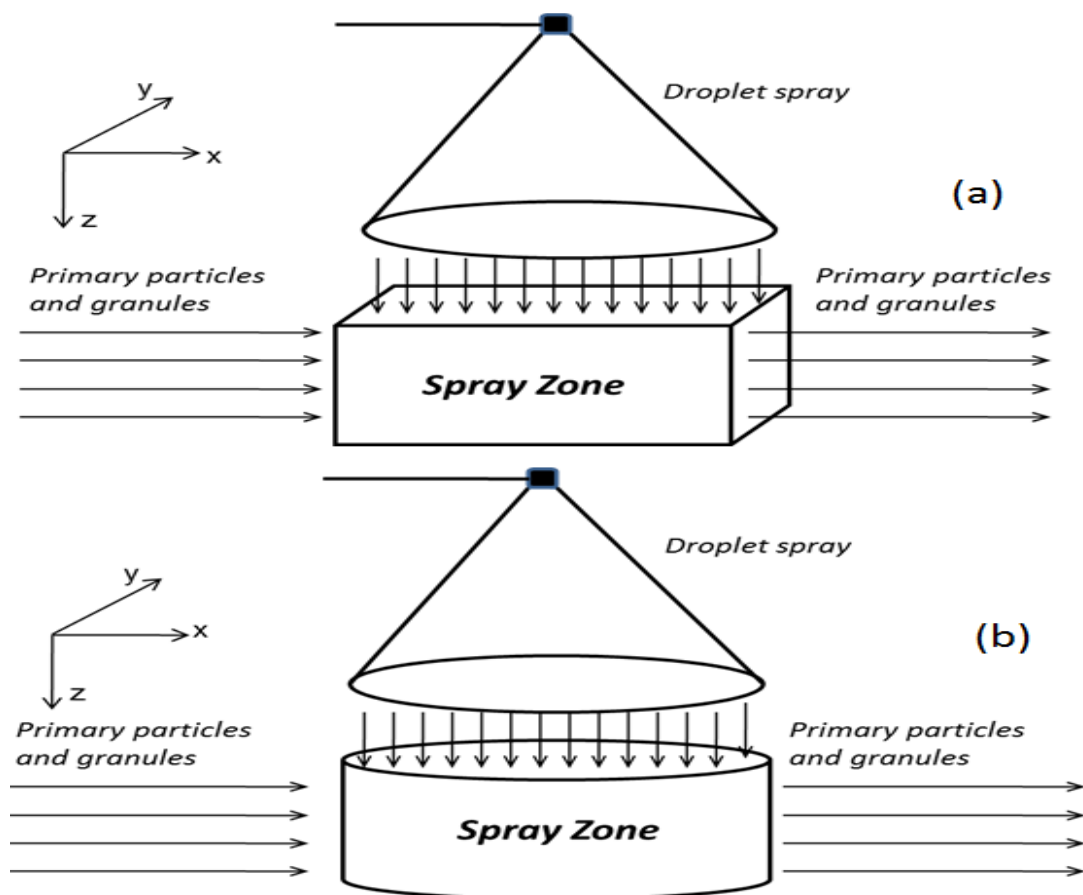


Figure 1

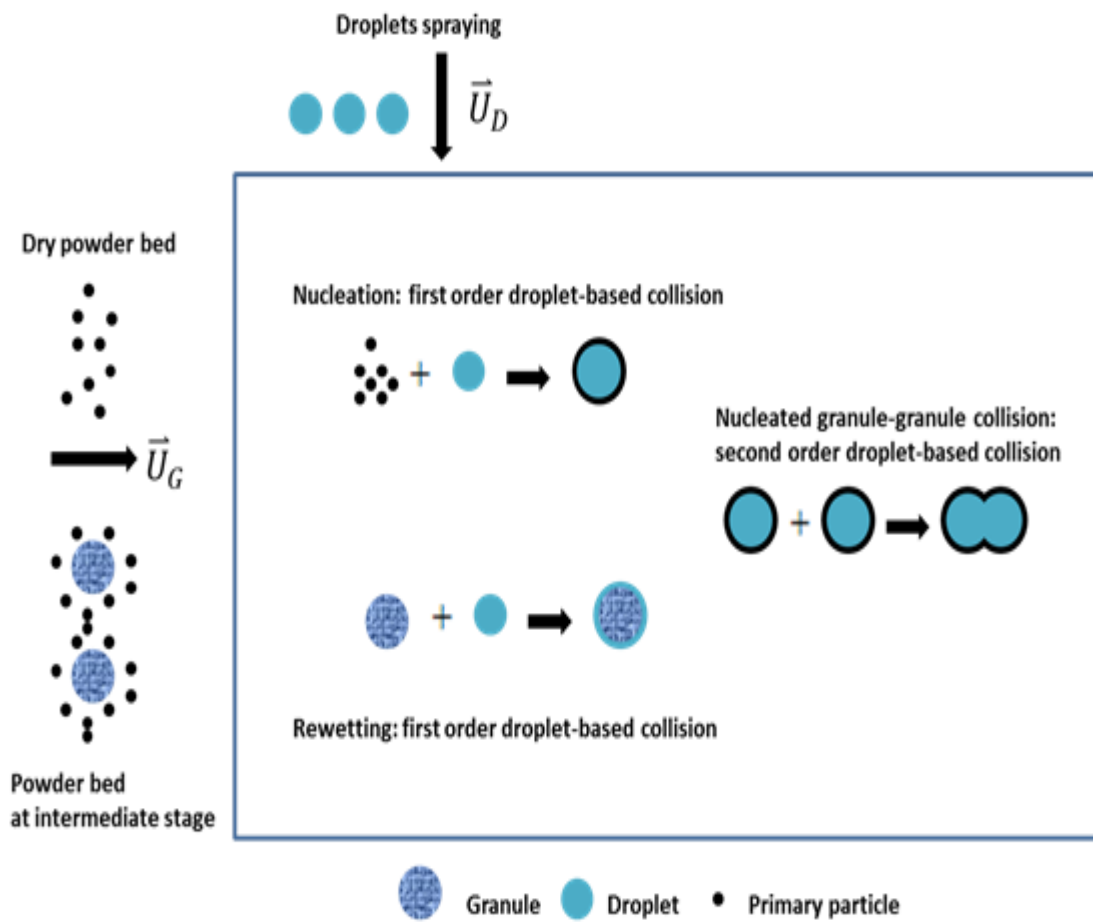


Figure 2

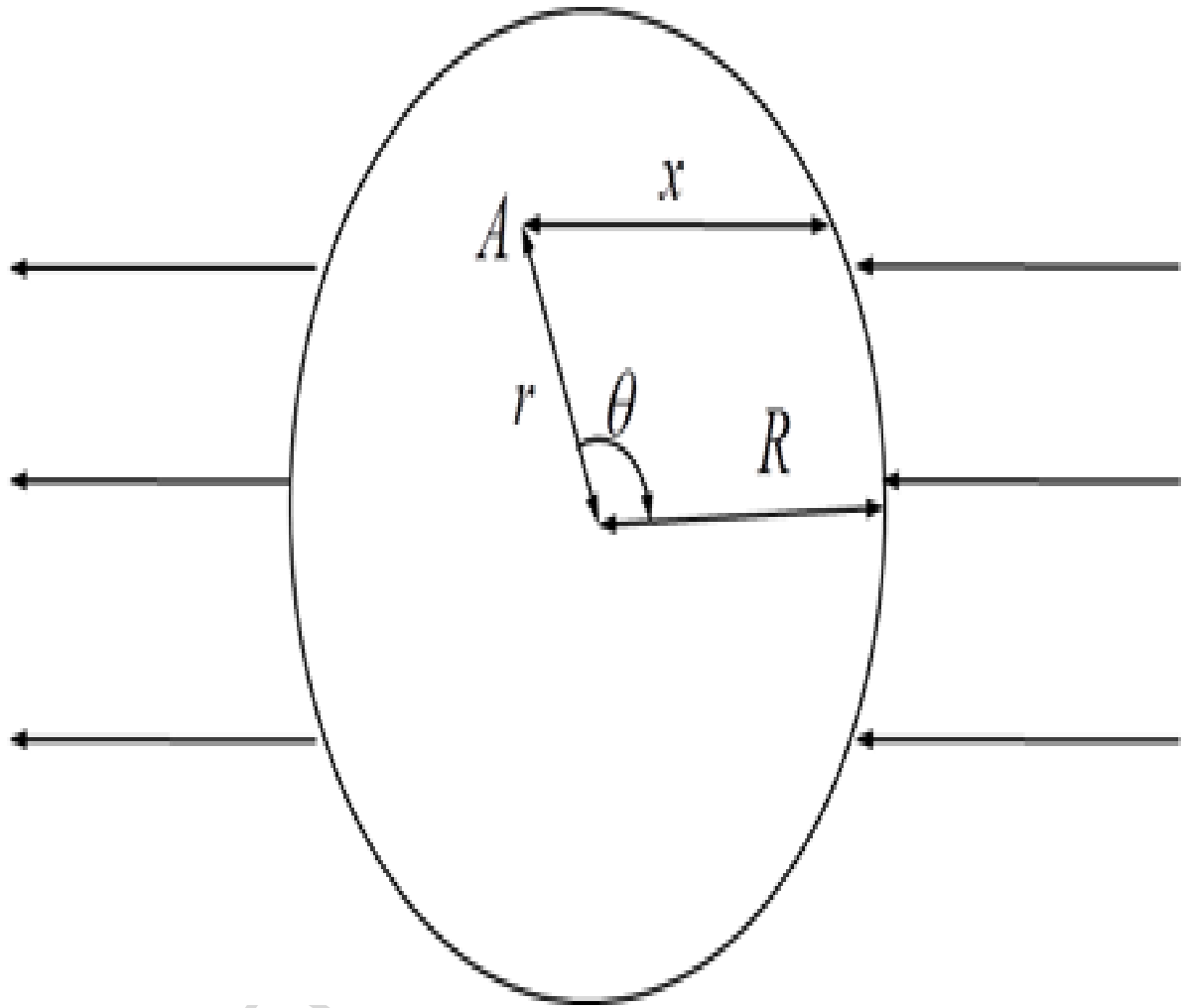


Figure 3

ACCEPTED

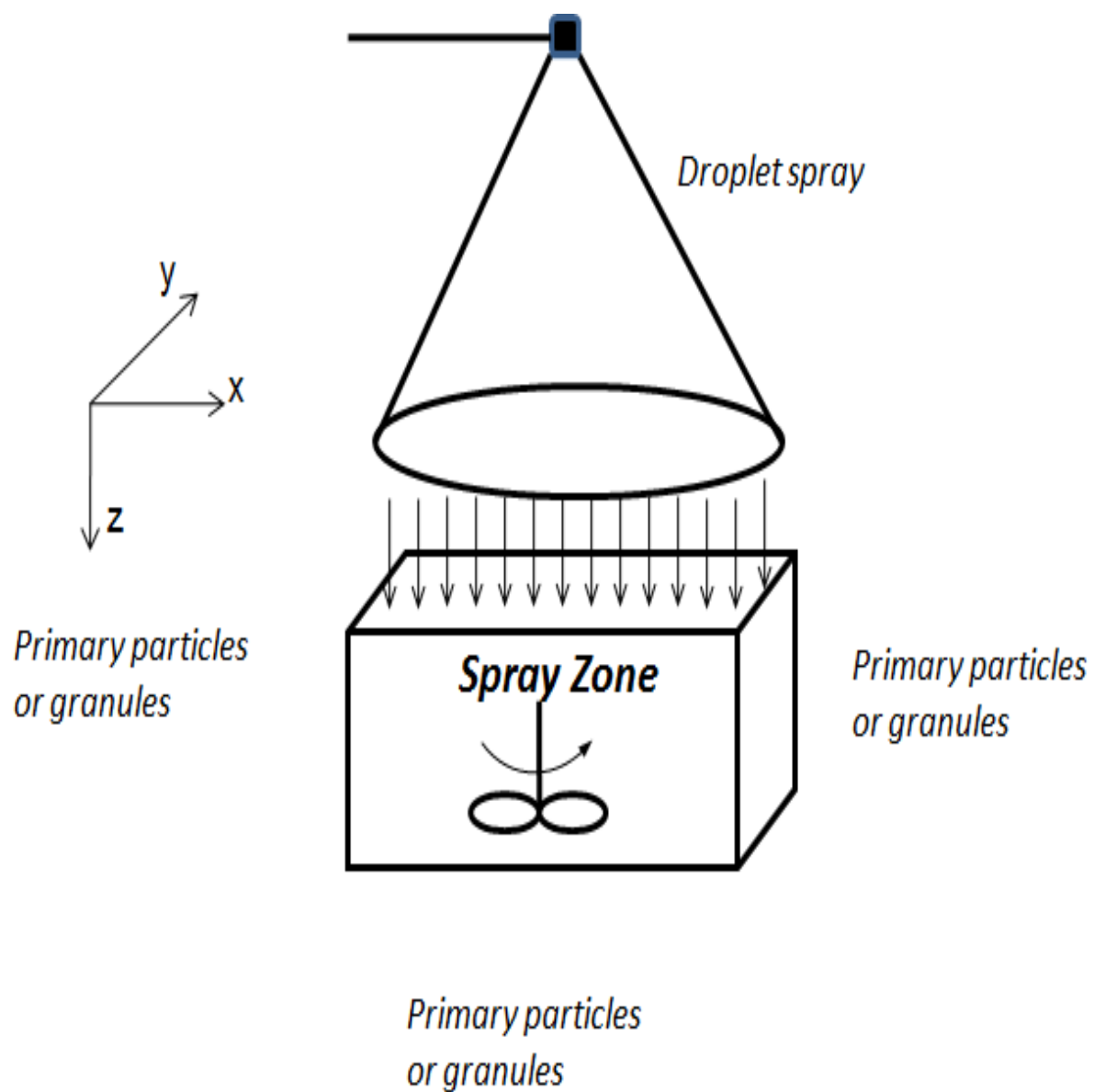


Figure 4

A

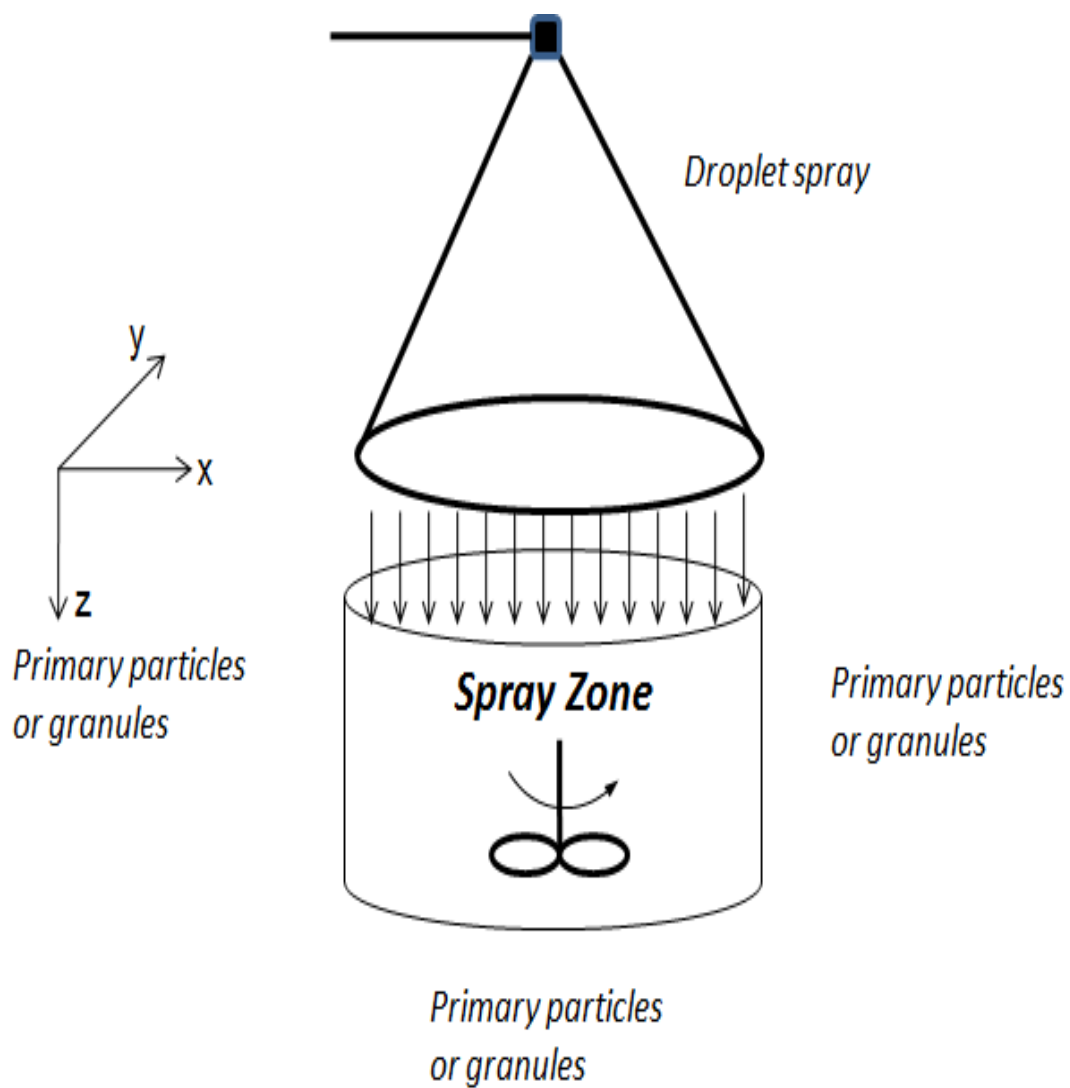
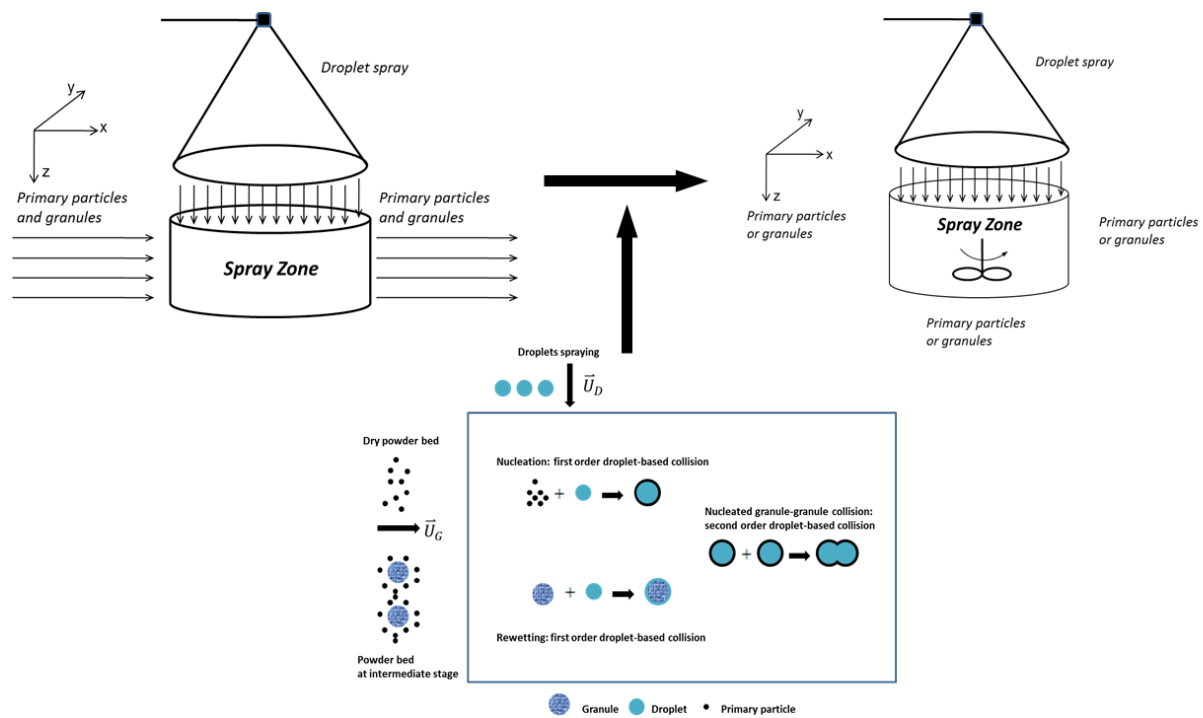


Figure 5

ACC



Graphical abstract

Highlights

- Spray zone with cross flow is quantified as a well-mixed compartment.
- Granulation kinetics are quantitatively derived at both particle and spray zone scale.
- Two spatial decay rates are defined to simplify the deduction.
- The depth of the spray zone is determined in both cuboid and cylinder shape.
- A real formulation case is used to estimate the size of the spray zone.